ELSEVIER

Soil Dynamics and Earthquake Engineering 19 (2000) 41–53

SOIL DYNAMICS AND EARTHQUAKE ENGINEERING

www.elsevier.com/locate/soildyn

Relationship between geomorphological land classification and site amplification ratio based on JMA strong motion records

F. Yamazaki[a,*], K. Wakamatsu[a], J. Onishi[b], K.T. Shabestari[a]

[a]*Institute of Industrial Science, The University of Tokyo, 4-6-1 Komaba, Meguro-ku, Tokyo 153-8505, Japan*
[b]*Central Japan Railway Company (JR Tokai), 1-6-6 Yaesu, Chuo-ku 103-0028, Japan*

Abstract

The relationship between the amplification ratio of earthquake ground motion and geologic conditions at Japan Meteorological Agency (JMA) stations nationwide was examined to propose an estimation method of the amplification ratio that is applicable to entire Japan. The amplification ratios for the instrumental JMA intensity, as well as for the peak ground acceleration and velocity, were obtained from the station coefficients of the attenuation relationships using strong motion records measured at 77 JMA stations over a period of more than 8 years. A combined use of geomorphological land classification and subsurface geology was found to yield the best estimate of the site amplification ratio. This result suggests that these data, and hence the Digital National Land Information, which is a nationwide GIS database, may be conveniently used for the estimation of strong motion distribution over large areas in Japan.

Keywords: Strong motion records; Site amplification ratio; Attenuation relation; Geomorphological land classification; Peak ground acceleration; Peak ground velocity; Seismic intensity

1. Introduction

The estimation of a strong motion distribution is important in seismic design and retrofit of structures, damage assessment of urban structures, and analysis of earthquake damage data. In particular, considering the use of estimated strong motion distribution in damage assessment systems [1–3], it is desirable to have a simple method applicable to large areas based on generally available data.

The major factors that affect the strong ground motion are the source characteristics typically represented by the magnitude, the wave propagation path effect represented by the source-to-site distance, and the subsurface soil condition that governs the amplification ratio. A large number of studies have been carried out by various researchers in the world to correlate the site amplification and geological classification using observed seismic records (e.g. Technical Committee for Earthquake Geotechnical Engineering, TC4, ISSMFE [4]). However, due to the limitation of available strong motion data and corresponding geological data, together with regional differences in geology and geomorphology, a widely applicable relation has not yet been established.

Attenuation relations provide a convenient tool to estimate the strong ground motion using the magnitude, depth, source-to-site distance, and in some cases, soil conditions. The attenuation relations are often used in earthquake damage assessments and seismic hazard analyses. Molas and Yamazaki [5,6] and Shabestari and Yamazaki [7] have recently developed attenuation relationships for the peak ground acceleration (PGA), peak ground velocity (PGV), JMA (Japan Meteorological Agency) instrumental seismic intensity and response spectra using records from the JMA-87-type accelerometers. In these studies, the station coefficients, which represent the relative amplification of observation stations in the attenuation relationships, were employed to characterize the effects of site conditions.

Several recent studies in Japan on seismic zonation employed the geomorphological and geological information included in the Digital National Land Information (DNLI), which is a digital database for geographic information systems (GIS) and covers entire Japan with a $1 \times 1\ \mathrm{km}^2$ size mesh, as a method to estimate site amplification characteristics.

Matsuoka and Midorikawa [8] compared the average S-wave velocity (V_S) of a recording site, or AVS (d), to a certain depth d (m) from the surface, and the amplification ratios for PGA and PGV at 47 locations where strong motion records were obtained in the 1987 Chibaken-Toho-Oki earthquake [9]. As a result, they proposed formulae that predict the PGA and PGV amplification ratios with respect

* Corresponding author. Tel.: +81-3-5452-6390; fax: +81-3-5452-6389.
E-mail address: yamazaki@iis.u-tokyo.ac.jp (F. Yamazaki).

0267-7261/00/$ - see front matter
PII: S0267-7261(99)00032-9

Fig. 1. Location of 77 JMA recording stations of the JMA 87-type-accelerometers.

to hills of the Tertiary Period or earlier, in terms of AVS (10) and AVS (30), respectively. They also proposed an empirical method to estimate AVS (30) from the subsurface geology, geomorphology and elevation based on S-wave velocity data from 459 sites in the Kanto region and geomorphological data in the DNLI. Using these two relations, the amplification ratio for PGV can be estimated from the DNLI through AVS (30).

Fukuwa et al. [10] also proposed a method to predict site amplification ratios based on the DNLI using the results of earthquake damage assessment studies in Aichi Prefecture and Nagoya City. They determined the amplification ratios for PGA and PGV between the surface and the rock outcrop (corresponding to $V_S = 3$ km/s) from the regression analysis using elevation, geomorphology, subsurface geology from the DNLI. The strain-dependent non-linear effects were considered in the Fukuwa's study.

It should be noted that the two methods described above were developed based on soil and geomorphological data from specific regions in Japan (the Kanto and Nobi regions, respectively). Although the applicability of these methods to those respective regions has been demonstrated, a further study may be necessary for their applicability to other parts of Japan. Hence, there is a need for methods that can be applicable to the entire Japan to estimate strong motion distribution in seismic hazard and damage assessments. At present, the method by Matsuoka and Midorikawa [8] is used in the earthquake damage assessment systems of the National Land Agency [11] and the Fire Defense Agency [3] of Japan.

The instrumental seismic intensity [12], which replaces the conventional seismic intensity scale based on human perception, came into use as the official measure by the JMA from October 1996. Many seismometers, which monitor the instrumental seismic intensity, have been deployed all over Japan [3]. Hence, the JMA instrumental seismic intensity will be used more than other indices in the near future. Thus a research on the amplification ratio of the JMA intensity is necessary.

Under these circumstances, the present study aims to propose an estimation method for the amplification ratios that is applicable to the entire Japan. Comparing the relationship between geomorphological and geological conditions of the JMA stations nationwide and the amplification ratios determined from the attenuation equations based on the JMA strong motion records, the DNLI is employed to predict the amplification ratios for PGA, PGV and JMA intensity.

2. Method for estimation of site amplification ratio

2.1. Attenuation relationship and station coefficients

Molas and Yamazaki [5,6] used 2166 sets of two horizontal component records from 387 earthquakes observed from 1 August 1988 to 31 December 1993 by the JMA-87-type accelerometers at 76 JMA stations in Japan and constructed attenuation relationships for PGA and PGV. Adding data observed till 31 March 1996 by the same instruments, Shabestari and Yamazaki [7] developed an attenuation equation for the instrumental JMA intensity (I) and revised the PGA and PGV attenuation equations. The records used in the study are 3990 sets from 1020 earthquakes at 77 JMA free field stations (Fig. 1).

The following functions were used in the regression analysis:

$$\log_{10}\mathrm{PGA} = b_0^{\mathrm{A}} + b_1^{\mathrm{A}} M_{\mathrm{J}} + b_2^{\mathrm{A}} r - \log_{10} r + b_4^{\mathrm{A}} h + c_i^{\mathrm{A}} \quad (1)$$

$$\log_{10}\mathrm{PGV} = b_0^{\mathrm{V}} + b_1^{\mathrm{V}} M_{\mathrm{J}} + b_2^{\mathrm{V}} r - \log_{10} r + b_4^{\mathrm{V}} h + c_i^{\mathrm{V}} \quad (2)$$

$$I = b_0^{\mathrm{I}} + b_1^{\mathrm{I}} M_{\mathrm{J}} + b_2^{\mathrm{I}} r - 1.89\log_{10} r + b_4^{\mathrm{I}} h + c_i^{\mathrm{I}} \quad (3)$$

in which M_J is the JMA magnitude, r the shortest distance (km) to the fault plane, h the focal depth (km), b_0, b_1, b_2, and b_4 are coefficients determined by regression, c_i the station coefficient representing the site effect at site i. The superscripts A, V and I indicate the PGA, PGV, and instrumental JMA intensity, respectively.

The two-stage regression procedure proposed by Joyner and Boore [13] was employed in the regression analysis, considering the correlation between the magnitude and distance in the data. In this method, a dummy variable was used for each earthquake. The coefficients related to the distance (b_2, b_4) were determined in the first stage, and the coefficients related to the magnitude (b_0, b_1) were

Table 1
Summary of station coefficients for 77 JMA stations and classification of geology, geomorphology and ground conditions of JMA station

No	Station	Elevation (m)	Station coefficient			Age of deposit	Geomorphologic classification	Type of sediment and rock	Subsurface geology	Soil type	No of group of this study
			PGA	PGV	JMA intensity						
1	Abashiri	38	−0.374	−0.316	−0.756	Pleistocene	Terrace	Unconsolidated sediment	Sand and gravel, Volcanic ash	2	7
2	Ajiro	68	0.209	0.091	0.297	Neogene	Mountain	Talus	Basalt	1	11
3	Akita	2	−0.124	0.114	0.123	Holocene	Delta	Unconsolidated sediment	Mud	4	3
4	Aomori	3	0.140	0.218	0.438	Holocene	Delta	Unconsolidated sediment	Sand	4	4
5	Asahikawa	112	−0.347	−0.082	−0.310	Holocene	Alluvial fan	Unconsolidated sediment	Sand and gravel	3	5
6	Ashizuri	32	−0.148	−0.285	−0.587	Unknown	Mountain	Volcanic rock	Syenite	1	11
7	Choshi	28	−0.111	−0.080	−0.156	Pleistocene	Terrace	Unconsolidated sediment	Sand, Loam	2	7
8	Fukui	10	0.064	0.117	0.270	Holocene	Flood plain	Unconsolidated sediment	Mud	4	3
9	Fukuoka	14	0.066	0.132	0.309	Holocene	Delta	Unconsolidated sediment	Sand	3	4
10	Hachijojima	80	0.059	−0.010	0.060	Pleistocene	Volcanic foot	Volcanic rock	Volcaniclastic material	2	10
11	Hachinohe	28	0.282	0.000	0.348	Pleistocene	Terrace	Unconsolidated sediment	Sand and gravel, Volcanic ash	2	7
12	Hakodate	35	−0.121	−0.133	−0.163	Pleistocene	Terrace	Unconsolidated sediment	Sand and gravel, Volcanic ash	2	7
13	Hamada	21	−0.111	−0.277	−0.619	Neogene	Mountain	Volcanic rock	Andesite	1	11
14	Hamamatsu	33	−0.094	−0.107	−0.244	Pleistocene	Terrace	Unconsolidated sediment	Sand and gravel	2	7
15	Hikone	87	0.184	0.310	0.602	Holocene	Delta	Unconsolidated sediment	Mud	4	3
16	Hiroshima	−4	0.041	0.103	0.239	Holocene	Delta	Unconsolidated sediment	Sand, Clay	4	4
17	Iida	484	0.013	−0.109	−0.175	Pleistocene	Terrace	Unconsolidated sediment	Sand and gravel	2	7
18	Irozaki	55	−0.162	−0.239	−0.564	Neogene	Hills	Volcanic rock	Volcanic rock	1	9
19	Ishigakijima	6	−0.160	−0.122	−0.287	Pleistocene	Terrace	Unconsolidated sediment	Limestone	2	8
20	Ishinomaki	44	0.206	−0.089	−0.037	Neogene	Hills	Consolidated sediment	Conglomerate	1	9
21	Kagoshima	6	0.008	0.164	0.258	Holocene	Delta	Unconsolidated sediment	Sand	4	4
22	Kanazawa	0	−0.005	0.171	0.233	Holocene	Delta	Unconsolidated sediment	Mud	4	3
23	Katsuura	10	−0.013	−0.141	−0.170	Holocene	Sand dune	Unconsolidated sediment	Sand	3	2
24	Kawaguchiko	860	0.315	0.067	0.241	Pleistocene	Volcanic foot	Volcanic rock	Lava	1	10
25	Kobe	59	−0.005	0.017	0.057	Pleistocene	Terrace	Unconsolidated sediment	Sand and gravel, Sand, Clay	2	7
26	Kofu	274	0.086	0.095	0.266	Holocene	Alluvial fan	Unconsolidated sediment	Sand and gravel	3	5
27	Kumamoto	39	−0.028	0.040	0.133	Pleistocene	Terrace	Volcanic rock	Volcanic ash, Lava	2	6
28	Kushiro	33	0.562	0.339	0.924	Pleistocene	Terrace	Volcanic rock	Volcanic ash, Sand	2	6
29	Maebashi	112	−0.255	−0.205	−0.518	Holocene	Alluvial fan	Unconsolidated sediment	Sand and gravel	3	5
30	Maizuru	3	−0.009	−0.045	0.012	Holocene	Reclaimed land	Unconsolidated sediment	Sand	3	1
31	Matsue	21	0.074	0.065	0.092	Neogene	Hills	Weakly consolidated sediment	Sandstone	1	9
32	Matsumoto	610	−0.308	−0.246	−0.596	Holocene	Alluvial fan	Unconsolidated sediment	Sand and gravel	3	5
33	Matsushiro	431	−0.537	−0.690	−1.443	Unknown	Mountain	Consolidated sediment	Mudstone	1	11
34	Matsuyama	34	0.119	0.179	0.385	Holocene	Alluvial fan	Unconsolidated sediment	Sand and gravel	3	5
35	Mishima	22	0.015	0.040	0.031	Holocene	Alluvial fan	Unconsolidated sediment	Sand and gravel	3	5
36	Mito	30	0.299	0.148	0.394	Pleistocene	Terrace	Volcanic rock	Loam, Sand and gravel	2	6
37	Miyakojima	41	0.020	−0.074	−0.124	Pleistocene	Terrace	Unconsolidated sediment	Limestone	2	8
38	Miyazaki	7	−0.098	0.057	0.099	Pleistocene	Terrace	Unconsolidated sediment	Sand and gravel	2	7
39	Morioka	154	0.343	0.241	0.763	Pleistocene	Terrace	Weakly consolidated sediment	Sand and gravel	2	7
40	Murotomisaki	186	−0.009	−0.058	−0.135	Pleistocene	Terrace	Unconsolidated sediment	Sand and gravel, Mud	2	7
41	Nagoya	56	0.068	0.050	0.058	Pleistocene	Hills	Weakly consolidated sediment	Sand and gravel	1	9
42	Naha	28	−0.115	−0.019	−0.142	Neogene	Terrace	Consolidated sediment	Mudstone	1	8
43	Naze	4	0.145	0.244	0.543	Holocene	Delta	Unconsolidated sediment	Clay, Sand and gravel	4	3

Table 1 (*continued*)

No	Station	Elevation (m)	Station coefficient			Age of deposit	Geomorphologic classification	Type of sediment and rock	Subsurface geology	Soil type	No of group of this study
			PGA	PGV	JMA intensity						
44	Nemuro	26	−0.025	−0.189	−0.303	Pleistocene	Terrace	Unconsolidated sediment	Sand and gravel, Volcanic ash	2	7
45	Niigata	3	−0.055	0.149	−0.001	Holocene	Reclaimed land	Unconsolidated sediment	Sand	4	1
46	Nobeoka	20	−0.063	−0.223	−0.455	Palaeogene	Mountain	Consolidated sediment	Shale	1	11
47	Ofunato	37	0.275	−0.032	0.198	Pleistocene	Terrace	Unconsolidated sediment	Sand and gravel	1	7
48	Oita	5	−0.029	0.131	0.237	Holocene	Delta	Unconsolidated sediment	Sand, Mud	4	4
49	Okayama	17	0.116	0.034	0.165	Holocene	Flood plain	Unconsolidated sediment	Clay	4	3
50	Omaezaki	45	−0.148	−0.168	−0.400	Pleistocene	Terrace	Unconsolidated sediment	Sand and gravel	2	7
51	Onahama	5	0.023	0.054	0.065	Holocene	Delta	Unconsolidated sediment	Sand	4	4
52	Osaka	13	−0.313	−0.199	−0.542	Pleistocene	Terrace	Unconsolidated sediment	Sand and gravel	2	7
53	Oshima	76	0.069	−0.002	0.102	Holocene	Volcanic foot	Volcanic stone	Lava	2	10
54	Sakata	4	0.135	0.411	0.654	Holocene	Delta	Unconsolidated sediment	Mud	4	3
55	Sapporo	17	−0.284	−0.105	−0.378	Holocene	Alluvial fan	Unconsolidated sediment	Sand and gravel	3	5
56	Sendai	37	0.063	0.039	0.130	Pleistocene	Terrace	Weakly consolidated sediment	Sand and gravel	2	7
57	Shimonoseki	18	0.091	0.091	0.277	Holocene	Reclaimed land	Unconsolidated sediment	Sand	3	1
58	Shionomisaki	74	0.040	−0.094	−0.117	Pleistocene	Terrace	Unconsolidated sediment	Sand and gravel	2	7
59	Shizuoka	14	−0.161	−0.207	−0.318	Holocene	Alluvial fan	Unconsolidated sediment	Sand and gravel	3	5
60	Suttsu	33	−0.029	−0.136	−0.249	Neogen–Holocene	Terrace	Volcanic rock	Andesite, Lava	2	8
61	Takada	15	0.135	0.200	0.302	Pleistocene	Terrace	Unconsolidated sediment	Sand and gravel?Mud, Sand	2	7
62	Takayama	561	−0.217	−0.306	−0.661	Holocene	Alluvial fan	Unconsolidated sediment	Sand and gravel	3	5
63	Tanegashima	18	−0.371	−0.317	−0.744	Palaeogene	Terrace	Consolidated sediment	Sandstone	1	8
64	Tateyama	6	0.061	0.148	0.308	Holocene	Lowland between bars	Unconsolidated sediment	Sand, Mud	3	2
65	Tokyo	21	0.198	0.155	0.375	Pleistocene	Terrace	Volcanic rock	Loam	2	6
66	Tomakomai	7	0.277	0.213	0.519	Pleistocene	Terrace	Volcanic rock	Volcanic ash	2	6
67	Tottori	14	0.131	0.227	0.521	Holocene	Delta	Unconsolidated sediment	Mud	4	3
68	Toyama	10	−0.150	−0.179	−0.323	Holocene	Alluvial fan	Unconsolidated sediment	Sand and gravel?Sand, Mud	3	5
69	Tsu	−1	0.120	0.147	0.273	Holocene	Delta	Unconsolidated sediment	Sand	4	4
70	Urakawa	30	0.216	0.218	0.473	Pleistocene	Terrace	Volcanic stone	Volcanic ash	2	6
71	Utsunomiya	121	0.049	−0.028	−0.062	Pleistocene	Terrace	Weakly consolidated sediment	Sand and gravel, Loam	2	7
72	Uwajima	94	0.084	0.067	0.106	Mesozonic	Hills	Consolidated sediment	Alternation of sandstone/mudstone	1	9
73	Wajima	7	−0.137	−0.008	−0.093	Holocene	Delta	Unconsolidated sediment	Sand	3	4
74	Wakamatsu	212	−0.324	0.008	−0.725	Holocene	Alluvial fan	Unconsolidated sediment	Sand and gravel	3	5
75	Wakkanai	11	0.061	0.192	0.494	Holocene	Reclaimed land	Unconsolidated sediment	Sand	4	1
76	Yokohama	38	−0.088	−0.154	−0.367	Pleistocene	Terrace	Volcanic rock	Loam, Mud, Sand, Sand and gravel	2	6
77	Yonago	7	0.067	0.189	0.395	Holocene	Sand bar	Unconsolidated sediment	Sand, Sand and gravel	3	2

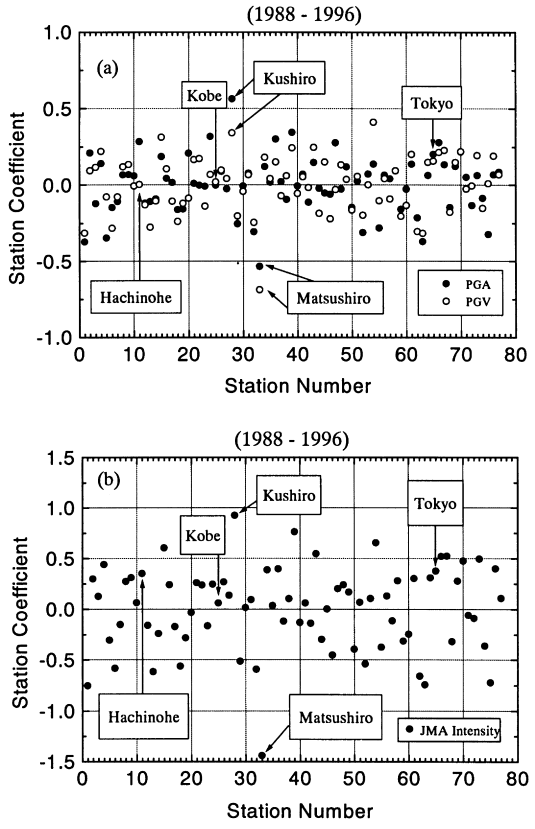

Fig. 2. Station coefficients for: (a) peak ground acceleration (PGA) and peak ground velocity (PGV): and (b) JMA intensity for 77 JMA stations.

determined in the second stage. Fukushima and Tanaka [14] also demonstrated the importance of this procedure.

Since the station coefficient is different for each station, the same number of dummy variables is also required. Thus, determination of the regression coefficients with the standard two-stage regression method would become difficult due to an excessive number of dummy variables, causing the singularity of the matrix. To solve this problem, a three-stage regression method, named the iterative partial regression was employed [5], and the coefficients were determined.

The station coefficient represents the site effect of the recording station as a supplement of the attenuation equation. The station coefficient may be affected by the geological and geomorphological conditions at the recording site and the conditions of the instrument, e.g. response characteristics of the instrument and its foundation. The mean of the station coefficients for all the recording stations is zero. Stations with positive station coefficients are supposed to have higher amplification ratio than the average site, while stations with negative station coefficients to have lower amplification.

Table 1 is a list of the station coefficients for the 77 JMA recording sites obtained by the analysis [7]. Fig. 2 plots these station coefficients with respect to the station number (Table 1). The station coefficient for PGA and JMA

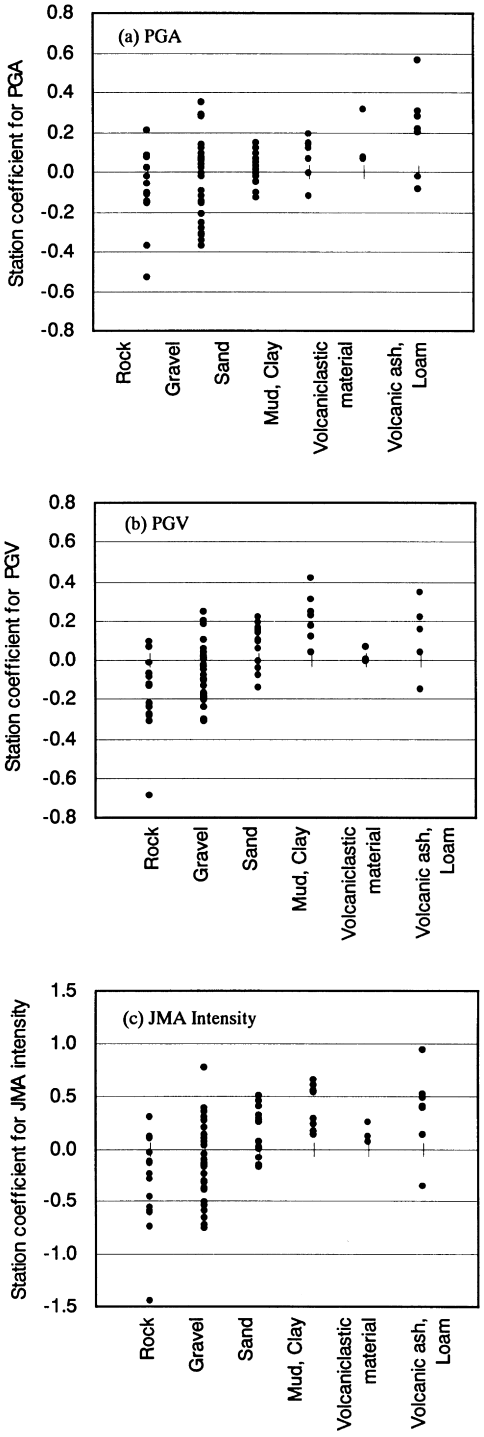

Fig. 3. Station coefficients for: (a) PGA; (b) PGV; and (c) JMA intensity with respect to the geomorphological classification at JMA stations.

intensity is largest for Kushiro and smallest for Matsushiro. It has been known that large acceleration is always recorded at Kushiro. This analysis proved the fact. Matsushiro is the only site where the instrument is placed in a rock tunnel. This fact explains the reason of the smallest station coefficient at this site. The station coefficients for PGV show similar tendency with those for PGA. The station with the

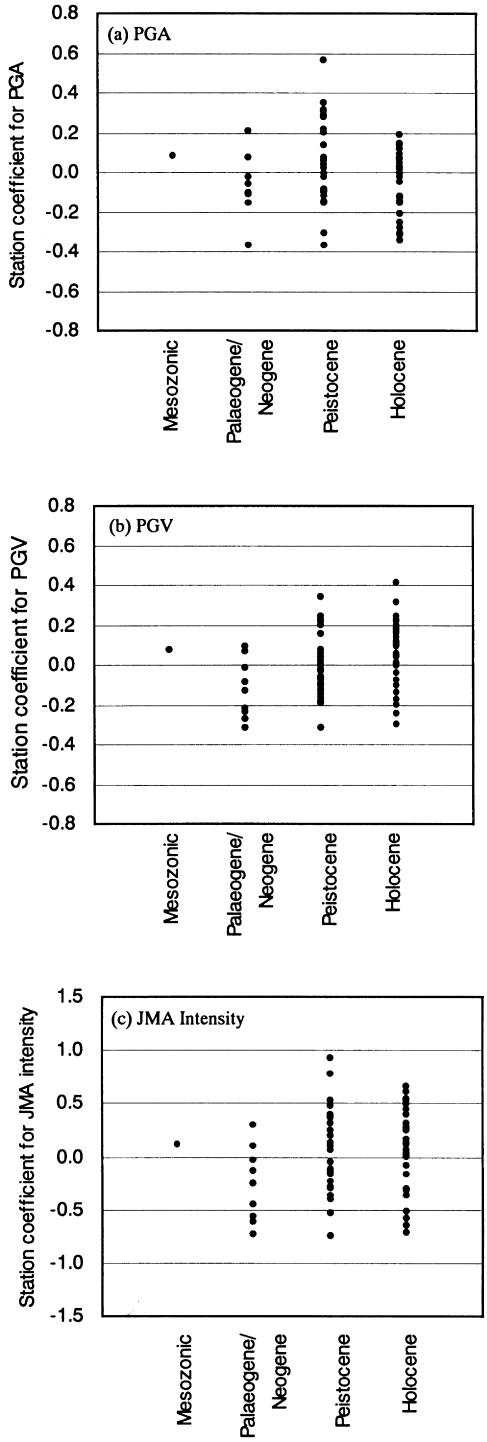

Fig. 4. Station coefficients for: (a) PGA; (b) PGV; and (c) JMA intensity with respect to the age of deposit at JMA stations.

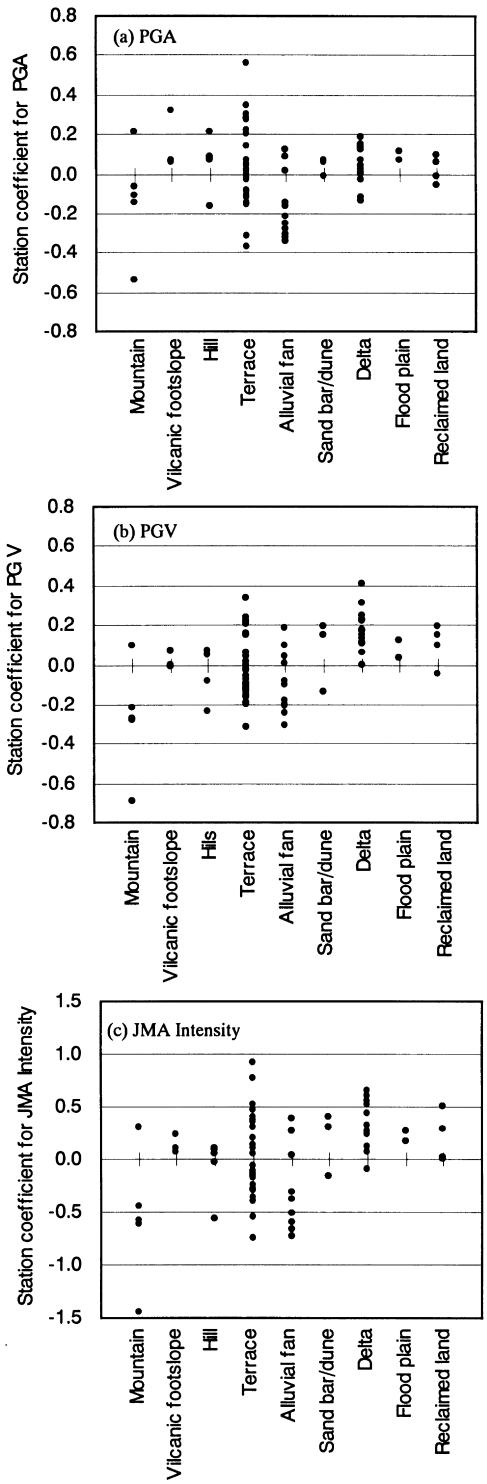

Fig. 5. Station coefficients for: (a) PGA; (b) PGV; and (c) JMA intensity with respect to the subsurface geology at JMA stations.

largest coefficient is Sakata, and the smallest coefficient is observed again in Matsushiro.

2.2. Conversion of station coefficient to site amplification ratio

If the peak ground acceleration at surface point *i* and that at the (hypothetical) outcrop beneath point *i* are represented by PGA_{Si} and PGA_{Bi}, respectively, the amplification ratio ARA_i of PGA at point *i* is given by

$$ARA_i = PGA_{Si}/PGA_{Bi} \quad (4)$$

Table 2
Correlation coefficient between the mean values of station coefficients in each classification and the station coefficients obtained by Shabestari and Yamazaki [7]

Method of classification	PGA	PGV	JMA intensity
Geomorphology	0.43	0.61	0.57
Age of deposit	0.22	0.36	0.30
Subsurface geology	0.47	0.64	0.61

The outcrop in this study is assumed as the surface of a stratum having sufficient rigidity (e.g. with V_S of at least 400 m/s). Then the supplement term (station coefficient) of the attenuation relation at the outcrop may have a constant value C_0^A. From Eq. (1), PGA_{Bi} at the outcrop is written as

$$\log_{10} PGA_{Bi} = b_0^A + b_1^A M_J + b_2^A r - \log_{10} r + b_4^A h + c_0^A \quad (5)$$

The peak ground acceleration at the ground surface is given by

$$\log_{10} PGA_{Si} = b_0^A + b_1^A M_J + b_2^A r - \log_{10} r + b_4^A h + c_i^A \quad (6)$$

The difference between Eqs. (5) and (6) yields

$$\log_{10}(PGA_{Si}/PGA_{Bi}) = c_i^A - c_0^A \quad (7)$$

From Eqs. (4) and (7), we obtain

$$ARA_i = 10^{C_i^A - C_0^A} \quad (8)$$

Similarly, the amplification ratio of the PGV is determined by

$$ARV_i = 10^{C_i^V - C_0^V} \quad (9)$$

Performing a similar operation on the amplification ratio of the JMA intensity, we get

$$ARI_i = c_i^I - c_0^I \quad (10)$$

From Eqs. (8)–(10), the amplification ratios for PGA, PGV and JMA intensity can be determined from their station coefficients. For the range of input motion in which soil non-linearity becomes significant, the site amplification ratios, especially for PGA, depends on the amplitude of ground strain. However, the attenuation relationships in this study were developed using the measured records. Since only few records are considered to be in the non-linear range, it would be difficult to introduce this effect to the amplification ratios.

In order to predict strong ground motion at non-recording sites, we must propose a method to estimate the station coefficient for those sites. The most influential factor determining the station coefficient may be the subsurface soil condition. Therefore, we will compare the station coefficients with the geological and topographical conditions of the recording sites hereafter.

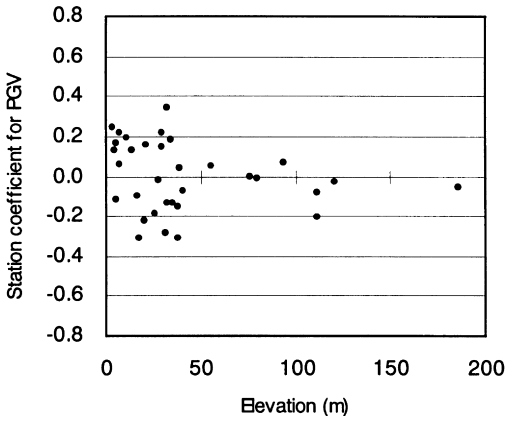

Fig. 6. Station coefficients for PGV with respect to the elevation of JMA stations located on terrace.

3. Relationship between ground conditions and station coefficients

3.1. JMA recording stations and ground conditions

To clarify the relationship between the ground condition and the station coefficient, it is necessary to investigate the geological conditions at the 77 JMA stations. To estimate site condition at the recording stations, which are distributed all over Japan, one feasible way would be the use of geomorphological and geological data compiled in the DNLI. Note that the geomorphological and subsurface geological data in the DNLI were made based on the geomorphological classification maps and subsurface geology maps of the region on a scale of 1/200,000 (1/100,000 scale only for Tokyo and Kanagawa Prefecture). This digital information gives the attributes of geomorphological and subsurface geological pixels, which account for the largest area in each pixel of the standard regional mesh (about 1×1 km^2), established by the Geographical Survey Institute of Japan. Therefore, although it is effective for the macroscopic determination of the average geomorphological and geological distribution over a large area, the DNLI may include some error in a case obtaining the geomorphological and geological conditions of a specific point, such as a recording station.

Thus, other means were used to determine the land classification of the recording stations. The geomorphological classification, age of deposit, type of the sediment, and subsurface geology were determined using the subsurface geology maps and geomorphological classification maps (published by the Economic Planning Agency and prefectures) from the Fundamental Land Classification Survey of Japan. The results are also summarized in Table 1.

3.2. Relationship between land classification and station coefficients

The relationships between the land classifications of JMA

Table 3
Classification of soil type in Japanese Highway Bridge Code [15]

Soil type	Geologic definition	Definition by predominant period
Type 1 (rock and hard soil)	Tertiary or older rock (defined as bedrock), of Pleistocene deposit with $H < 10$ m	$T_G < 0.2$ s
Type 2 (hard soil)	Pleistocene deposit with $H \geq 10$ m or Holocene deposit with <10 m	$0.2 \leq T_G < 0.4$ s
Type 3 (medium soil)	Holocene deposit with $H < 25$ m including soft layer with thickness less than 5 m	$0.4 \leq T_G < 0.6$ s
Type 4 (soft soil)	Other than above, usually soft Holocene deposit or fill	$T_G \geq 0.6$ s

stations and the station coefficients for PGA, PGV and JMA intensity were investigated. Fig. 3 shows the relationship between the geomorphological classification and the station coefficients for PGA, PGV and JMA intensity. With regard to PGV and JMA intensity, such tendency is observed that the harder the ground corresponding to the geomorphological classification, the smaller the station coefficient becomes. However, there is a great deal of scatter among the station coefficients within the same geomorphological classification. Hence, one can conjecture that the geomorphological classification alone is not the controlling factor of the station coefficient. Possible reasons for this scatter include the following: (1) the influence from other factors, such as the deep ground structure of the site, may be significant; (2) the recording stations classified as a geomorphologic unit do not present the standard ground condition for the unit; and (3) a large difference in the vertical soil profile may be associated with the same geomorphological classification. A more detailed classification may be necessary for

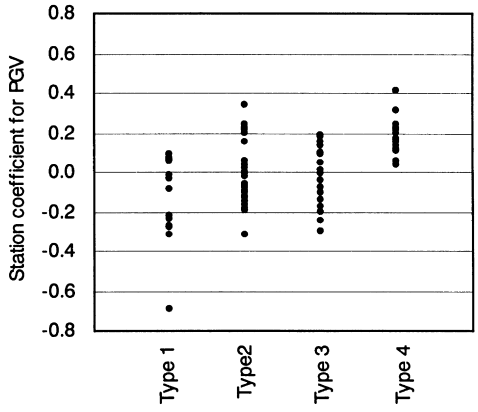

Fig. 7. Station coefficients for PGV with respect to the soil-type classification of JMA sites.

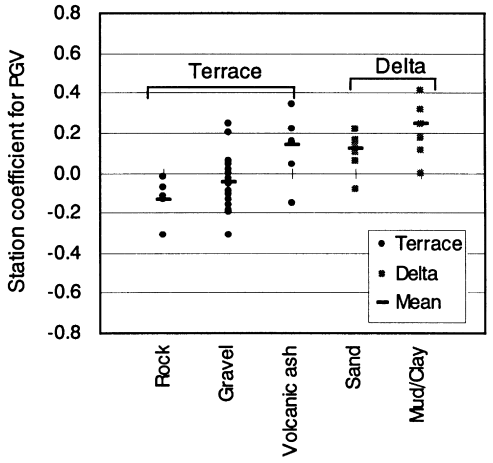

Fig. 8. Effect of subsurface geology in a geomorphologic classification with respect to the station coefficient for PGV.

the geomorphologic units with a large scatter in the station coefficient.

Fig. 4 shows the relationship between the geological periods and the station coefficients for three indices. Practically no correlation is seen for any of these indices. Hence, it would be difficult to estimate the station coefficient using only the geological period.

Fig. 5 shows the relationship between the subsurface geology and the station coefficients for three indices. In the geologic classification, lava is included under volcaniclastic (pyroclastic) material as this is a type of volcanic rubble. Loam in Japan, which is a kind of volcanic cohesive soil, is combined with volcanic ash. In the figure, all of the station coefficients exhibit a rising trend in the order of rock, gravely soil, sandy soil, clayey soil, volcaniclastic material and volcanic ash (order of smaller particle size); that is, the softer the ground, the larger the amplification ratio becomes.

Table 2 shows the coefficients of correlation between the actual station coefficients and the average values of station coefficients in the same group according to three types of land classification (geomorphological classification, geological period, and subsurface geology). In each of the station coefficients (those for PGA, PGV, and JMA intensity), the correlation coefficient was largest in the classification by subsurface geology, and second largest in that by geomorphology.

3.3. Relationship between elevation and station coefficients

Matsuoka and Midorikawa [8] and Fukuwa et al. [10] considered the elevation as a factor in the estimation of the site amplification ratio. Hence, we also examined the relationship between elevation and the station coefficient. The relationship was studied for each geomorphological classification, in order to minimize the influence of other factors. As an example, Fig. 6 shows the relationship between the elevation and the station coefficient for PGV at the stations classified as terraces. Practically no

Table 4
Average station coefficient and amplification ratios for eleven groups in this study

No	Groups of this study	Number of stations	Average of station coefficient			Amplification ratio		
			PGA	PGV	JMA intensity	PGA	PGV	JMA intensity
1	Reclaimed land	3	0.009	0.065	0.096	1.31	2.12	0.65
2	Sand bar, sand dune	3	0.038	0.065	0.178	1.40	2.12	0.73
3	Delta (mud, clay)	8	0.081	0.203	0.389	1.54	2.92	0.94
4	Delta (sand)	8	0.029	0.118	0.216	1.37	2.39	0.77
5	Alluvial fan	11	−0.166	−0.092	−0.286	0.87	1.48	0.27
6	Terrace (volcanic ash)	7	0.205	0.137	0.350	2.05	2.50	0.90
7	Terrace (sand and gravel)	18	−0.005	−0.053	−0.064	1.26	1.62	0.49
8	Terrace (rock)	5	−0.131	−0.134	−0.309	0.95	1.34	0.24
9	Hill	5	0.054	−0.029	−0.069	1.45	1.71	0.48
10	Volcanic foot	3	0.148	0.018	0.134	1.80	1.91	0.69
11	Mountain	3	−0.107	−0.261	−0.554	1.00	1.00	0.00
Correlation coefficient		74	0.602	0.705	0.684			

correlation can be found between them. Categories other than terraces were also studied in the same way, but correlation was again not found. A possible reason for this may be explained as follows.

As stated before, the previous studies [8,10] were conducted for specific regions of Japan (the Kanto and the Nobi plains). If dealing with a single fluvial plain, such as the above regions, the composition of sediment differs upstream to downstream of the river, even with the same geomorphology. In a single alluvial fan, the further downstream you go, the finer the sediment becomes. Matsuoka and Midorikawa [8] considered the effect of change in the characteristics of sediment by elevation. However, this kind of geomorphological principle cannot be applicable for a nationwide study such as the present one, which covers a large number of river basins.

3.4. Relationship between soil type and station coefficients

Classification of ground by soil type has been used in the field of civil engineering. The relationship between the soil type classification [15] shown in Table 3 and the station coefficient was investigated. The soil types of the 77 JMA stations were primarily determined from their geomorphological classification. Boring data were needed to distinguish between soil types 3 and 4. Thus, if boring data revealed that the thickness of the Holocene deposit was equal or more than 25 m, the station was considered to be soil type 4, and if not, it was considered to be soil type 3.

Fig. 7 shows the relationship between the soil type and station coefficient for PGV. A large amount of scatter is observed in the station coefficient within the same soil type. However, the average values of the station coefficients increase in the order of type 1 to type 4. That is, the softer the ground, the higher the seismic response becomes as has already been pointed out in the previous papers [5–7].

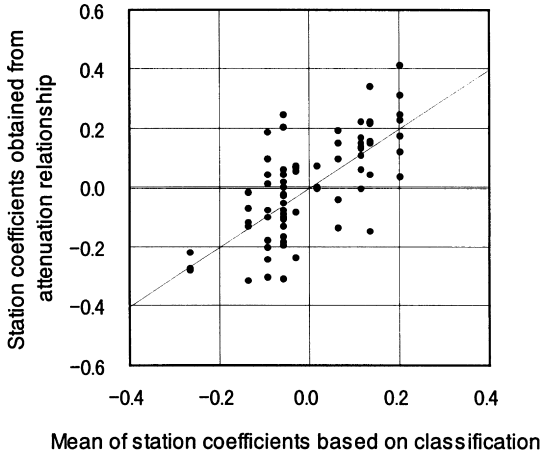

Fig. 9. Mean of the station coefficients based on the classification in this study for PGV compared with the station coefficients obtained from the attenuation relationship proposed by Shabestari and Yamazaki [7].

4. Relationship between land classification and site amplification ratio

The relationships between various geological, geomorphological and soil conditions and the station coefficients were investigated above. It was found that a great deal of scatter exists in the relationship if each attribute is considered individually. However, considering the use of amplification ratios in the estimation of seismic motion distribution over a large area, we will develop a method to predict amplification ratios based on land classification. Land classification can be estimated using the DNLI in Japan, without using information difficult to obtain, such as boring data and predominant periods.

Among the land classifications discussed above, the correlation coefficients for subsurface geology and geomorphological classification were relatively high in Table 2. Therefore, we investigated differences in the station coefficients due to the difference in subsurface geology in the same geomorphological classification as shown in Fig. 8.

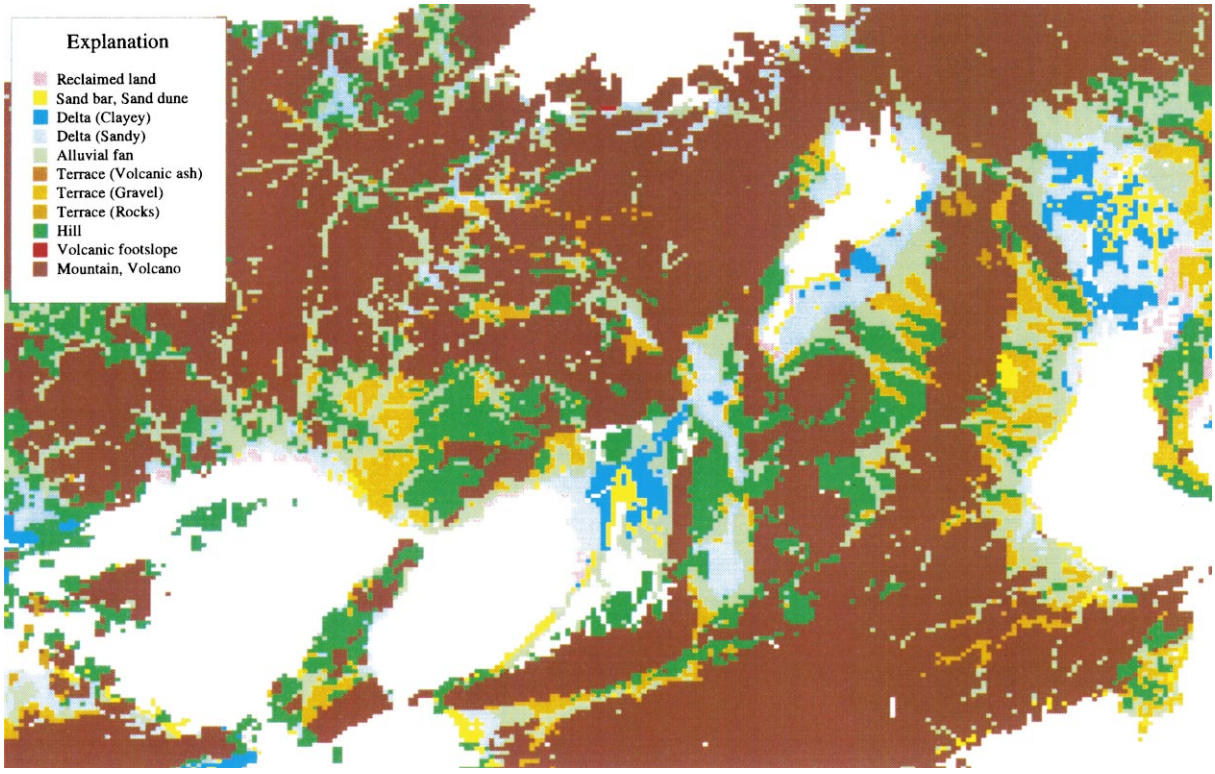

Fig. 10. Distribution of 11 soil groups proposed in this study for the Kinki region evaluated from the Digital National Land Information.

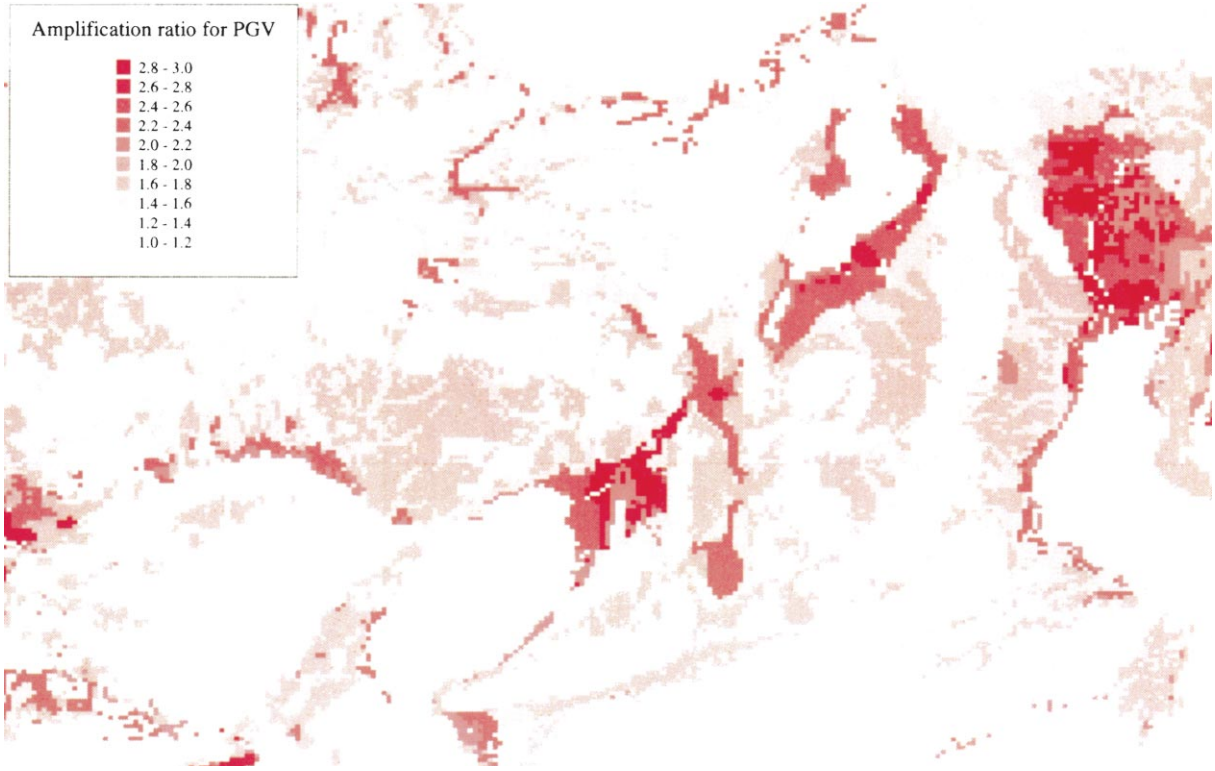

Fig. 11. Distribution of the predicted amplification ratio for PGV in the Kinki region.

Table 5
Geomorphological classification and subsurface geology in the Digital National Land Information corresponding to the 11 groups in this study (Amplification ratio for JMA intensity is defined as the difference between the intensity at ground surface and that at bedrock)

No	Groups of this study	Geomorphologic classification in Digital National Land Information	Subsurface geology in Digital National Land Information
1	Reclaimed land	Reclaimed land, Reclaimed land/ polder	Sand, Sandy soil
2	Sand bar, sand dune	Natural levee, Natural levee/Sand bar, Lowland between sand dunes, Sand dune	Sand, Sandy soil, Dune sand
3	Delta (mud, clay)	Reclaimed land, Delta, Flood plain	Mud, Muddy soil, Silt, Clay, Peat
4	Delta (sand)	Reclaimed land, Delta, Flood plain	Sand, Sandy soil, Sand and Mud, Alternation of sand and mud
5	Alluvial fan	Alluvial fan, Volcanic fan	Gravel, Gravelly soil, Sand and gravel
6	Terrace (volcanic ash)	Loam terrace, Shirasu terrace, Volcanic sand terrace	Volcanic ash, Loam, Pumice flow deposit, Shirasu,
7	Terrace (sand and gravel)	Sand and gravel terrace	Gravel, Gravelly soil, Sand and gravel
8	Terrace (rock)	Rock terrace, Limestone terrace	Rock
9	Hill	Hill, Volcanic hill	Rock
10	Volcanic foot	Volcanic footslope, Lava flow field, Lava plateau	Volcaniclastic material, Lava, Mud flow deposit
11	Mountain	Mountain, Mountain footslope, Volcano	Rock, Volcanic rock

The subsurface geology of terrace was divided into the groups of rock, sand/gravel, and volcanic ash. The average values of the station coefficients for each group were found to increase in the order of rock, sand/gravel and volcanic ash for the three strong motion indices. Thus, the three-group subdivision was adopted for the terrace. The subsurface geology of delta was divided into two groups, sandy soil and clayey soil, as also shown in Fig. 8. The average value of the station coefficients is higher for the clayey soil group than that for the sandy soil group with respect to PGA, PGV, and JMA intensity. Hence, this subdivision for delta was adopted. The geomorphological classifications other than delta and terrace, namely mountain, hill, alluvial

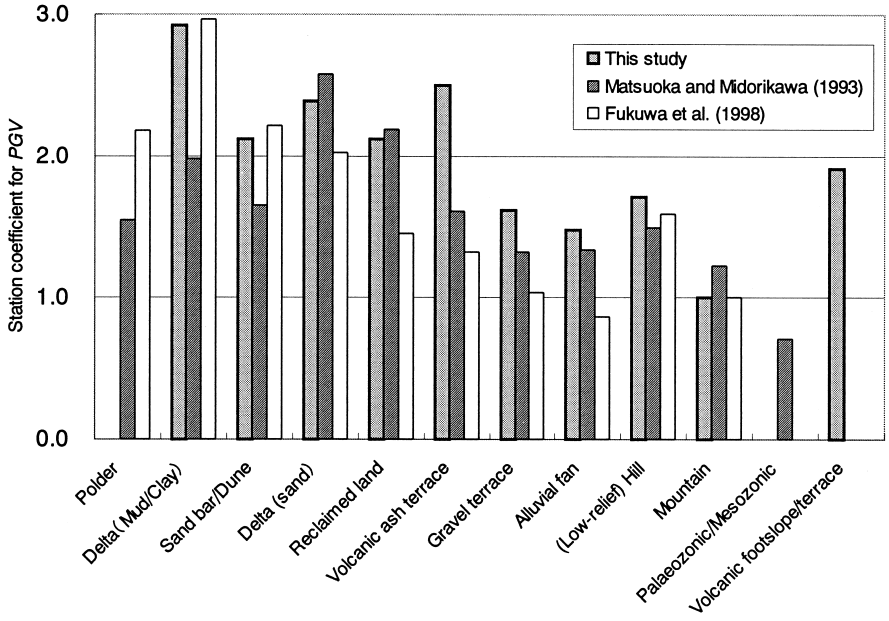

Fig. 12. Comparison of amplification ratios for PGV proposed in this study and two previous studies.

fan, sand bank/dune, and reclaimed land, could not be subdivided because the subsurface geology was of the same composition in each classification.

Based on these considerations, the geomorphological classification was used as the major class and then subdivided into groups according to subsurface geology, as shown in Table 4. Note that the geomorphological classification considers the geomorphological origin, topography, material composition, and time of formation, thus resulting in the consideration of age of deposit as well. The result of classification of the 77 JMA stations into the 11 groups is listed in Table 1.

Table 4 also shows the average station coefficients in each group, the number of recording stations used to calculate the average values, and the correlation coefficient between the average values and the actual station coefficients. In determining the average station coefficient for each group, three stations (Matsushiro, Ajiro and Wakkanai) were omitted. The instrument of Matsushiro (mountain) is placed in a rock tunnel and that of Ajiro (mountain) is located on talus (colluvial deposit) ground. These conditions significantly differ from those for other stations. Therefore, these station coefficients look like singular points in Figs. 2 and 3. Wakkanai station (reclaimed land) is located on a small-scale reclaimed land area built adjacent to a mountainous area. This condition was judged to be different from that for ordinary reclaimed lands in Japan, due to the reason that the bedrock lies in a shallow depth.

The correlation coefficient between the average values of the station coefficients in a group and the actual station coefficients is highest for PGV (0.705) and lowest for PGA (0.602). This tendency has also been seen in the other classifications described before.

The average values in each of the 11 groups categorized by geomorphology and subsurface geology are proposed as the estimation of the station coefficients. Fig. 9 shows the relationship between these values and the actual station coefficients. Even though geomorphology is combined with subsurface geology, considerable variation is still seen in the estimation of station coefficients.

Table 4 also shows the amplification ratios, converted from the average values of station coefficients in the table. The ground surface in the regions geomorphologically classified as mountain is considered to be close to the rock outcrop. Then the conversion is performed so that the amplification ratio of the mountain group is set as 1.0 (for JMA intensity, set as 0.0). Table 5 shows geomorphological and subsurface geological categories in the DNLI corresponding to the 11 groups in this study. Using Table 4 and the DNLI, it is possible to estimate the site amplification ratios throughout Japan by 1×1 km^2 pixel.

The distribution of amplification ratio for PGV is provided as an example for a rectangular area of the Kinki region (centered by Osaka and Kobe) with 270 km east–west and 180 km north–south directions (total of 41,266 pixels). The geomorphology and subsurface geology of the area were obtained from the DNLI, and the results were converted to the 11 categories of this study (Fig. 10). Then, the amplification ratio of PGA, PGV, and JMA intensity were determined on the basis of those 11 categories as shown in Fig. 11 for PGV.

5. Comparison of the results with the previous studies

The amplification ratio for PGV obtained in this study (Table 4) was compared with the results of two previous studies [8,10]. Both the studies by Matsuoka and Midorikawa [8] and Fukuwa et al. [10] considered the elevation in estimating the site amplification ratio. For the purpose of comparison, elevation values should be assigned to each of the geomorphological and subsurface geological categories used in this study. Using the elevations at the 77 JMA stations, the average elevations for each geomorphological and subsurface geological category were calculated and they were used in the estimation Eqs. (8) and (10). A unified definition of the bedrock was also needed to compare the amplification ratios from the three studies. Matsuoka and Midorikawa's study proposes amplification ratios, taking the hill of the Neogene period or earlier as a reference point. We assumed that this reference point is almost equivalent to our reference ground "mountain" and a direct comparison was made. Since Fukuwa's study considered the bedrock with $V_s = 3$ km/s as a reference point, the amplification ratios proposed by Fukuwa were divided by 1.45, which is the amplification ratio for mountainous ground in his study.

Fig. 12 compares the amplification ratios for PGV by the three studies. All the three estimation methods provide basically the same tendencies in the relative amplification in each geomorphological and geological category. The absolute values of the converted amplification ratios are also similar in spite of the fact that the three studies used completely different seismic records and ground data in deriving the amplification ratios. However, non-trivial differences are still observed for some soil categories. A further study using more comprehensive data set, e.g. from K-NET [16] with 1000 recording sites nationwide, is suggested.

As stated before, the estimation of amplification ratios of strong motion indices from geomorphology and subsurface geology alone may be associated with considerable variability. Thus, the use of the proposed amplification ratios should be limited for the gross estimation of seismic motion over a large area.

We are currently expanding the proposed relation to response spectra. The period-dependent station coefficients from the spectral attenuation [6] can also be estimated based on geomorphology and subsurface geology. The results of this research will be presented in a separate paper.

6. Conclusion

A method for estimation of site amplification characteristics in Japan from generally available data was investigated considering its use in earthquake damage assessments for large areas. The station coefficients in the attenuation equations for PGA, PGV and JMA instrumental seismic intensity, based on the strong motion records measured by the JMA-87-type-accelerometers, were compared with land classifications by the Fundamental Land Classification Survey and others. After several trials, the scatter of station coefficients within each soil group was minimized when the 77 JMA stations are divided into 11 soil groups based on their geomorphological classification and subsurface geology.

From the average values of the station coefficients in each group, the site amplification ratios for the strong motion indices were obtained taking a mountainous ground in the geomorphological classification as the reference. Then the amplification ratios for PGA, PGV and JMA intensity can be estimated by 1×1 km^2 pixels throughout Japan using the geomorphological and subsurface geological data in the DNLI of Japan. A comparison with two previous studies showed relatively close results for the PGV amplification ratios, irrespective of the differences in the methods and data used.

A further study using more comprehensive strong motion data sets, for example, from K-NET, may improve the accuracy of the proposed relations between the site amplification and land classification.

References

[1] Whitman RV, Anagnos T, Kircher C, Lagorio HJ, Lawson RS, Schneider P. Development of national earthquake loss estimation methodology. Earthquake Spectra 1997;13(4):643–61.

[2] Eguchi R, Goltz JD, Seligson HA, Flores PJ, Blais NC, Heaton TH, Bortugno E. Real-time loss estimation as an emergency response decision support system: the early post-earthquake damage assessment tool (EPEDAT). Earthquake Spectra 1997;13(4):815–32.

[3] Yamazaki F, Noda S, Meguro K. Developments of early earthquake damage assessment systems in Japan. In: Balkema AA, editor. Structural safety and reliability, Proceedings of ICOSSAR'97, 1998. p. 1573–80.

[4] Technical Committee for Earthquake Geotechnical Engineering, TC4, ISSMFE. Manual for zonation on seismic geotechnical hazards, 1993.

[5] Molas GL, Yamazaki F. Attenuation of earthquake ground motion in Japan including deep focus events. BSSA 1995;85(5):1343–58.

[6] Molas GL, Yamazaki F. Attenuation of response spectra in Japan using new JMA records. Bulletin of Earthquake Resistant Structure Research Center, Institute of Industrial Science, University of Tokyo 1996;29:115–28.

[7] Shabestari KT, Yamazaki F. Attenuation relationship of JMA seismic intensity using JMA records. Proceedings of the 10th Japan Earthquake Engineering Symposium, Kobe, 1998. p. 529–34.

[8] Matsuoka M, Midorikawa S. GIS-based integrated seismic hazard mapping for a large metropolitan area. Proceedings of the Fifth International Conference on Seismic Zonation 1995;II:1334–41.

[9] Architectural Institute of Japan. The Off East Coast of Chiba Prefecture Earthquake, 17 December 1987. Digitized Strong-Motion Earthquake Records in Japan Vol. I. 1992.

[10] Fukuwa N, Arakawa M, Nishizaka R. Estimation of site amplification factor using Digital National Land Information. Journal of Structural Engineering 1998;44(B):77–84 (in Japanese).

[11] Okayama K. Earthquake disaster countermeasures in Japan. Proceedings of the First Asia-Pacific Workshop on Research Coalition for Urban Earthquake Disaster Management, Earthquake Disaster Mitigation Research Center, RIKEN, 1998. p. 9–17.

[12] Shabestari KT, Yamazaki F. A Proposal of new seismic intensity scale compatible with MMI evaluated from seismic records. 11th European Conference on Earthquake Engineering, CD-ROM, 1998.

[13] Joyner WB, Boore DM. Peak horizontal acceleration and velocity from strong-motion records including records from the 1979 Imperial Valley California, earthquake. BSSA 1981;71:2011–38.

[14] Fukushima Y, Tanaka T. A new attenuation relation for peak horizontal acceleration of strong earthquake ground motion in Japan. BSSA 1990;80(4):757–83.

[15] Japan Road Association. Specifications for Highway Bridges Part V Earthquake Resistant Design, 1980.

[16] Kinoshita S. Kyoshin Net (K-NET). Seismological Research Letters 1998;69(4):309–32.